Applied Acoustics 224 (2024) 110102

Contents lists available at ScienceDirect

Applied Acoustics

journal homepage: www.elsevier.com/locate/apacoust

Design and validation of a comprehensive model to characterize sonic crystals acoustic screens in the low frequency regime

L. Onrubia-Fontangordo, J.M. Bravo Plana-Sala, S. Castiñeira-Ibáñez *, J.V. Sánchez-Pérez

Centro de Tecnologías Físicas, Universitat Politècnica de València, Camino de Vera, s/n, Valencia, 46022, Spain

ARTICLE INFO

Keywords:
Environmental noise
Noise barriers
Sonic crystals
Numerical models
Experimental prototype

ABSTRACT

In this paper, we present a comprehensive model to obtain numerical/experimental results on the acoustic behaviour of sonic crystals in the low frequency range (up to 1700 Hz). We have focused our attention on this range because it is the most difficult to control in the field of environmental acoustics, and sonic crystals are particularly useful for this purpose. The immediate application is the design of high-tech acoustic screens for traffic noise, although sonic crystals are capable of screening any type of noise due to their scalability. In addition, the model can be used for the analysis of the rich physical behaviour of these metamaterials at these frequencies. The model, completely designed and developed by us, consists of a three-dimensional numerical simulation software together with a real prototype to obtain experimental results. It is precisely the joint use of these two tools that gives our model a unique versatility. To validate the model in this low frequency range, we have considered different sonic crystals where their geometrical parameters, lattice and filling factor have been varied. The accurate results obtained, compared with those obtained in anechoic chamber and with those calculated with other existing numerical models, show that our model works successfully. All this in a simple and low-cost way compared to other existing design techniques and other ways of obtaining experimental results.

1. Introduction

Noise as an annoying and disruptive element of health and rest has been documented for more than 130 years [1]. Today, prolonged exposure to high levels of environmental noise is one of the leading causes of ill health in Europe. In terms of health, such exposure to environmental noise is directly linked to negative effects such as discomfort, difficulty of falling asleep, cardiovascular and metabolic system impairment or learning disabilities in children [2]. Traffic noise exposure has been classified as the second-greatest environmental health threat after air pollution [3].

At the European level, it is estimated that 113 million people are subjected to the influence of traffic noise. Within this number, 22 million are severely affected by noise, 6.5 million have severe sleep disorders and 48 000 have developed cardiovascular diseases [4]. More than 420 000 km of the main European roads –which also have more than 3 million annual trips– present noise problems to be solved [3]. Within this scenario, the European Union has set a goal for the year 2030 to reduce the number of people affected by traffic noise by 30% using noise control mechanisms [5].

Among the mechanisms that are most used for controlling traffic noise are policies that allow progress in the electrification of the current fleet of vehicles [6], use of special rolling noise-reducing asphalts [7], stricter speed limits on certain stretches of road [8], and the use of acoustic barriers [9].

The use of acoustic barriers is especially important when it is not possible to act directly on the source of noise. It is often the case on highways and highways, where vehicles travel at high speeds, generating high levels of ambient noise. In those cases, it is necessary to act on the noise transmission channel. Although acoustic barriers perform reasonably well in the middle and high frequency range, their performance decreases significantly when they have to work in the low frequency range.

There are different types of technologies for sound attenuation through the use of acoustic barriers. Traditional barriers are the most used, studied and developed. They consist of a continuous obstacle interposed between the noise source and the receiver [10]. Noise attenuation capacity is basically determined by the geometric characteristics of the barrier itself (length, thickness, height) and its relative location

* Corresponding author.
E-mail addresses: luonfon@doctor.upv.es (L. Onrubia-Fontangordo), jobrapla@fis.upv.es (J.M. Bravo Plana-Sala), sercasib@fis.upv.es (S. Castiñeira-Ibáñez), jusanc@fis.upv.es (J.V. Sánchez-Pérez).

https://doi.org/10.1016/j.apacoust.2024.110102
Received 7 March 2024; Received in revised form 22 May 2024; Accepted 2 June 2024

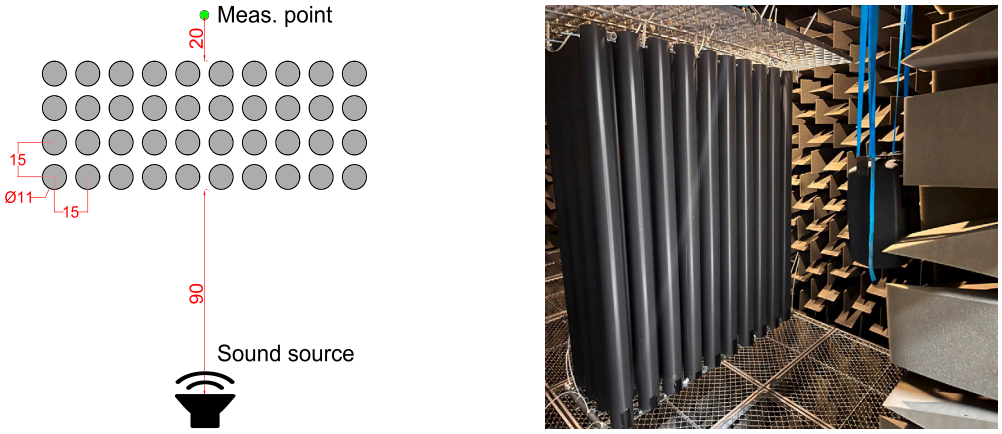

Fig. 1. (Left) Diagram in top view of the SC placed in the anechoic chamber where the emission and the measurement points can be observed, dimensions in cm. (Right) Photograph of the SC placed in its measurement position in the chamber in front of the sound source.

between source and emitter, which affects the acoustic diffraction at its upper edge [11]. In recent years, novel acoustic metamaterials called Sonic Crystals (SCs[1]), which are formed by arrays of acoustic scatterers in air, are used to design a new generation of high-tech acoustic barriers [12]. These barriers base their operation on the physical principle of multiple scattering [13], and are usually called Sonic Crystal Acoustic Screens (SCAS[2]).

The geometry and spatial arrangement [14] of the scatterers that compose the SCAS will generate band gaps –or forbidden frequency bands– that will prevent the transmission of the sound wave through them. This opens the possibility of creating a "tunable" barrier to attenuate the most problematic frequency bands, such as low frequencies. Within the forbidden bands, SCAS obtain higher acoustic attenuation values than traditional barriers [15].

Generally, the design of a SCAS is carried out with the support of two- or three-dimensional numerical simulation tools (depending on the available computing power). These tools help researchers to adjust the barrier to the noise spectrum to be attenuated. Once the numerical calculations have been performed, the next step is to test its acoustic performance on a smaller scale in a controlled environment, such as an anechoic chamber. In this way, the results of the numerical models are verified. If the numerical and experimental data agree, the production phase of the barrier could follow.

In general, not everyone has the possibility of carrying out anechoic chamber testing and measurements, which impedes the verification of SCAS and thus increases the uncertainty of their use. Even when a suitable chamber is available for this purpose, the complexity of the set-ups and their price can be a problem. Works such as that of Qin et al. [16], where a full-scale SCAS has been built and tested on a real stretch of highway, evidence the high material and time costs of this type of installation and the importance of robust prototyping procedures.

In this paper, we present a comprehensive model to obtain accurate numerical and experimental data about the performance of SCs in the low frequency range. Its main use is to design technologically advanced SCAS, although it is also possible to use it as a tool to study the physics involved in these metamaterials or to design another kind of advanced devices based on SCs. The first element of our work is a 3D numerical model based on the existing ones [17], but much more developed. The model serves as a basis for the development of an experimental prototype, which constitutes the second part of our work. This prototype uses scatterers with their actual diameter and achieves sound attenuation results in agreement with those obtained in an anechoic chamber. The proposed model allows obtaining numerical and experimental results under controlled conditions in a fast and economical way, with respect to other methods. The comprehensive model has been checked with a battery of SCs with designs that cover different geometrical SC parameters, using square and triangular lattice scatterer arrangements, as they are the most commonly used in SCAS designs [18–20]. The experimental prototype also provides great versatility by working with scatterers of a reduced size (in its length, as the diameter stays in actual size) which can be 3D printed to any type of design and specification.

2. Materials and methods

As already mentioned, the starting point for the design of a SCAS is the simulation of the SCs. This is performed using numerical tools validated by the scientific community such as the Finite Element Method (FEM), Finite-Difference Time-Domain (FDTD) or Boundary Element Method (BEM). These simulation procedures allow the study of SCAS at a low cost and in a versatile way. Once a design that is best suited for the noise spectrum to be attenuated is found, it would be validated in the anechoic chamber. This is done to verify the behaviour of the design in a more realistic environment. In this work, a new simulation model is proposed as a basis for the development of an experimental prototype.

This section presents the initial experimental set-up, consisting of a SC in a square lattice arrangement placed in an anechoic chamber, which serves as the validation reference. Then, the conventional 2D and 3D models are shown and the characteristics of a customized novel 3D numerical model are explained. Finally, a new experimental prototype, which allows the theoretical models to be verified cheaply and easily, is presented.

2.1. Anechoic chamber measurements

As mentioned above, in the process of validating the results from the numerical simulation, the anechoic chamber is generally used in an attempt to recreate the real behaviour of the barrier in an outdoor environment but under controlled conditions.

For our work, the measurements were carried out in the anechoic chamber belonging to the Universitat Politècnica de València. For this purpose, an array of 1.5 m tall cylindrical PVC scatterers is used. The array, as can be seen in Fig. 1, is formed with 4 rows and 10 columns of scatterers in a square lattice arrangement. The outer diameter of the scatterers is 11 cm and the lattice constant is 15 cm, thus obtaining a Bragg frequency (f_{bragg}) of 1 145 Hz, considering a propagation speed of 343 m/s.

[1] From now on, SC stands as the abbreviation for Sonic Crystal and SCs as the abbreviation for Sonic Crystals.

[2] From now on, SCAS stands as the abbreviation for Sonic Crystal Acoustic Screen.

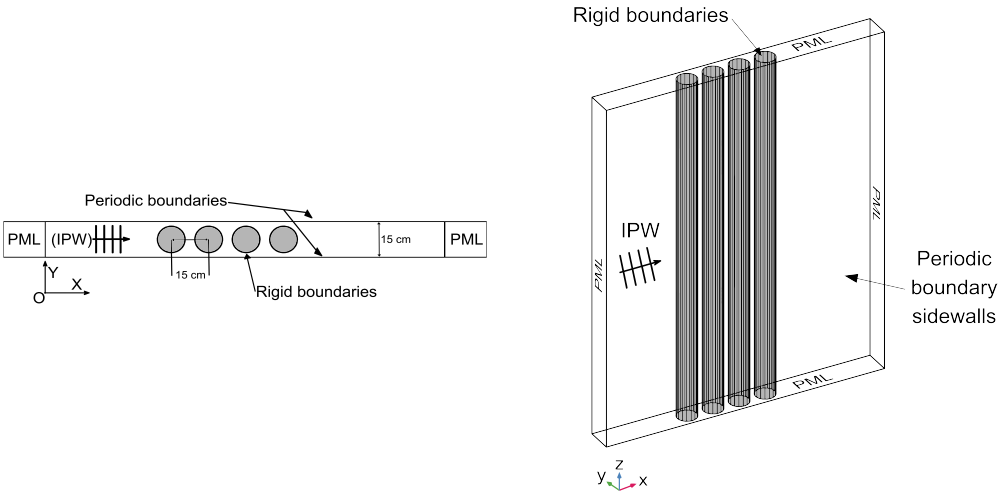

Fig. 2. (Left) Two- and (Right) three-dimensional models used in previous works to predict the behaviour of a 4-row, infinite-column SCAS.

Given the nature of the measurements, any kind of incident signal could be used, but we have used continuous white noise for all tests, both experimental and numerical. In this case, continuous white noise has been generated from a GENELEC 8040A directional sound source and measuring the unweighted sound spectrum (in FFT form) between 100 and 1 700 Hz at the point indicated above with a prepolarised free-field $^1/_2''$ Brüel & Kjær Type 4189 microphone. This allows a clear view of the first band gap around the Bragg frequency. The Insertion Loss parameter (IL) has been used throughout the work as a metric to measure the attenuation of the different samples, and can be defined as the difference of the acoustic pressure in the same point with and without the sample.

$$IL = L_{empty} - L_{SCAS}, \tag{1}$$

where L_{empty} represents the sound pressure level as a function of frequency without the SCAS and L_{SCAS} is the sound pressure level with the SCAS.

The IL measured in an anechoic chamber is considered to be a SCAS behaviour closer to reality than the ideal numerical model calculations. This is due to the fact that edge diffraction effects occur in anechoic chambers which are not taken into account by the ideal numerical models.

2.2. Previous numerical models

In recent years, simplified 2D and 3D ideal models representing the propagation of an incident plane wave on a SC with lateral periodicity boundary conditions and no diffraction at the edges have been used for the design of SCAS [21–23].

In this paper, these models have been implemented using COMSOL Multiphysics® software version 6.1 with the acoustics module, and adjusted to the geometry of the SC used in the reference measurements.

The 2D model uses periodic boundary condition in its lateral walls, thus recreating an infinite-column SC with finite rows, as the distance between the side boundaries is equal to the lattice constant of 15 cm. The considered domain consists of a 160 cm long by 15 cm wide rectangle where the SC, modelled as a rigid boundary (a boundary that represents a nearly infinite acoustic impedance) with a diameter of 11 cm, is placed. A plane wave propagating along the positive OX axis is used as a sound source, and PMLs [24] are placed in both ends of the domain in order to prevent unwanted reflections (see Fig. 2). Simulation frequency is the 100 to 1 700 Hz range with a mesh of 6 elements per wavelength, giving a total of 5 600 degrees of freedom and a calculation time of 25 seconds on our computer.

The 3D model has the same geometry as the 2D one, but with an added 200 cm height. The model uses the same periodic boundary condition in its lateral walls, and a similar plane wave propagating along the OX axis as a sound source. This time, PMLs are not only placed at the ends of the model, but also at its top and base in order to prevent reflections from occurring in any of these areas. Simulation frequency range stays the same as the 2D model, as well as the number of mesh elements per wavelength, the added height raises the number of degrees of freedom to 238 000 and the calculation time is 1 hour on our computer.

2.3. Proposed numerical model

The development of this new numerical model has a dual purpose. On the one hand, the achievement of a better approximation of the prediction in comparison with the measurements in an anechoic chamber. On the other hand, to serve as a guide in the development of a prototype that allows measurements to be carried out that yield results comparable to those obtained in an anechoic chamber, but on a smaller scale and without the necessity for a complex installation.

The proposed numerical model tries to eliminate certain ideal conditions of the previous models, like replacing the lateral periodicity conditions by parallel rigid boundaries or replacing the plane wave radiation with a point source (similar to the radiation of a loudspeaker) that is closer to the measured anechoic reality. The dimensions of the scatterers and the lattice topology reproduce the values already described in the anechoic chamber measurements in Fig. 1 left.

2.3.1. Square lattice model

The model consists of two distinct components. First, an emission chamber where the scatterers, consisting of rigid contours, are placed at a distance of 50 cm from the emission surface. This surface, which is depicted in Fig. 3, has been modelled in such a way that represents the membrane of a loudspeaker moving with a normal acceleration of 1 m/s^2 in the positive direction of the OX axis. On the other hand, the receiving chamber is formed by absorbing boundaries, modelled with PMLs and its geometry has been designed trying to eliminate parallelism to reduce the influence of eigenmodes. In this reception chamber is where the measurement points will be placed, their position is set 20 cm away from the surface of the last scatterer, in the centre of gravity of the transverse surface. This replicates the measurement configuration of the anechoic chamber.

The method used for the simulation is the finite element method (FEM) using COMSOL Multiphysics® software version 6.1 with the acoustics module. The frequency range of simulation is 100 to 1 700

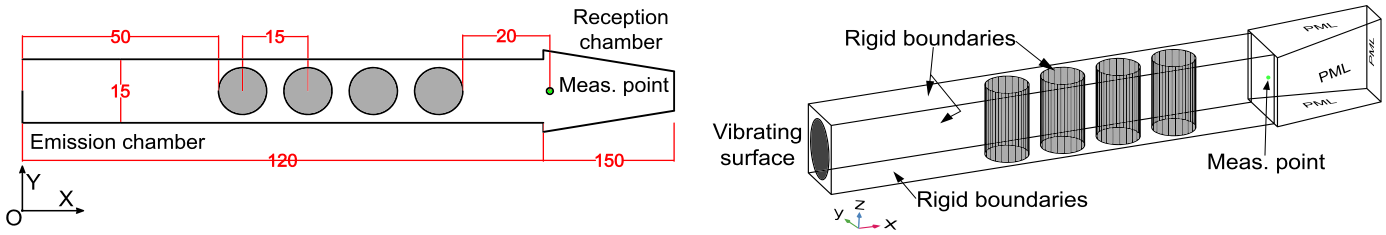

Fig. 3. (Left) 2D top view and dimensions (in cm) of the proposed numerical model. (Right) 3D view of the numerical model and boundary conditions used.

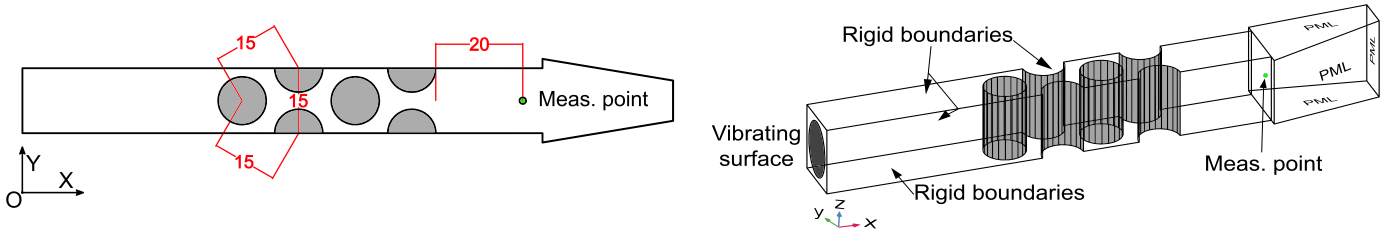

Fig. 4. (Left) 2D top view of the triangular lattice model. (Right) 3D view of the triangular lattice model and boundary conditions used.

Hz, with a mesh of 6 elements per wavelength, giving a total of 41 500 degrees of freedom and a calculation time of 9 minutes on our computer.

2.3.2. *Triangular lattice model*

To further validate the experimental prototype, an additional model with a triangular lattice SC is used. This model is largely the same as the previous model in section 2.3.1 but with a triangular arrangement of the scatterers.

The model maintains the same geometry and dimensions of the emission and reception chambers, as well as the position of the first scatterer respective to the emission surface. The measuring point is considered at the same 20 cm distance to the last scatterer surface (see Fig. 4). The frequency range of simulation is the same 100 to 1 700 Hz as before. A mesh of 6 elements per wavelength was used, giving a total of 42 100 degrees of freedom and a calculation time of 7 minutes on our computer. Note that in this case, the use of perfect semi-cylinders to maintain periodicity conditions on the side walls of the domain is mandatory.

2.4. *Proposed experimental prototype*

The validation of IL results in an anechoic chamber has some major drawbacks. For example, the scatterers that make up the SC are large, and the test set-up is costly and complicated. On the other hand, access to an anechoic chamber is generally not possible for everyone. The creation of this experimental prototype is intended to provide an alternative to these complex tests.

As already mentioned, the starting point is the numerical model described in the previous section 2.3 and the aim is to ensure that the behaviour of the prototype coincides with the results obtained in the test carried out in the anechoic chamber.

The numerical model envisaged a rigid boundary condition on all side surfaces, floor and top of the enclosure. To be as close as possible to the numerical model, this condition is recreated using a solid outer frame (outer walls, floor and removable ceiling) of 17 mm thick MDF wood. A 22 mm thick flat hardwood (oak) board is added to the interior side walls to adjust the lattice constant of the system to the exact size of the simulations (see Fig. 5). This ensures that the inner side walls are parallel to each other at a constant distance of 15 cm, which matches the anechoic chamber and numerical model SC lattice parameters. With the use of a removable inner side wall, the lattice constant can be adjusted to other values by varying the board thickness.

The end section of the prototype is prepared as a reception chamber. In the numerical model, PML conditions are established for the reception chamber boundaries. In the prototype, an attempt is made to recreate these conditions using thick wedges of closed cell acoustic foam. We have characterised this material by obtaining its absorption coefficient (α) in an impedance tube, obtaining reasonable values in the frequency range considered (0.9 maximum and 0.5 minimum). However, as the materials used in the prototype are not perfect absorbers, the combination of absorbing material together with the use of a non-parallel walls has been used in order to avoid the appearance of unwanted reflections and standing waves in the reception chamber.

Emission characteristics of the numerical model consider a vibrating surface with the same geometry as that of the loudspeaker used in the prototype. In order to match the measure point used in the numerical model (which is located 20 cm away from the last scatterer) a centred rod is used to accurately position the microphone.

During measurements, the system is closed with top covers. To guarantee air-tightness of the system, sealing strips are used on all exposed surfaces of the prototype that are in contact with the top lids, clamps are used to ensure a consistent seal.

The scatterers used in the prototype correspond geometrically to the numerical model and their position, with the first scatterer 50 cm away from the loudspeaker, corresponds to the simulated conditions. The material of the scatterers chosen to match the stiffness conditions of the model is PVC, the same material used in the SC measured in the anechoic chamber. However, the length of the scatterers is 20 cm, compared to the 150 cm of each scatterer used in the anechoic chamber. The height of the scatterers, in the prototype, is precisely adjusted to the height of the prototype chamber to avoid leaving a gap between the end of the scatterer and the lid.

Thus, the objective proposed at the beginning of the section is achieved by reducing the amount of material required by 98.6% compared to the anechoic chamber measurements. It also simplifies assembly and allows greater control of the position and parallelism of the scatterers. On the other hand, its dimensions and ease of assembly open up the possibility of its use for any SC-based acoustic barrier design team.

With all this, not only does it achieve savings, but it also introduces the advantage of 3D printing of the scatterers, which makes it possible to work with complex geometries.

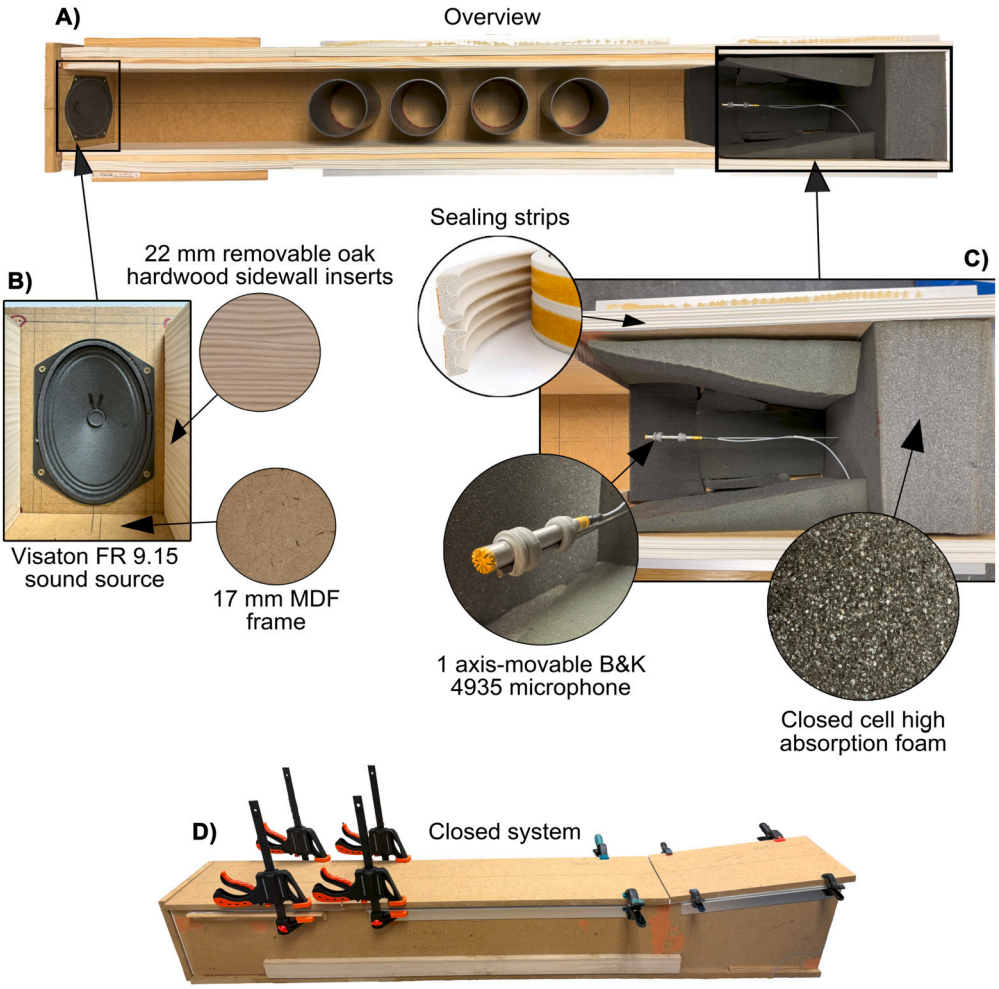

Fig. 5. (A) Top view of the experimental prototype. (B) Detail of the sound source used in the prototype. (C) Various details of the reception area of the prototype. (D) View of the prototype with the lids closed for taking measurements.

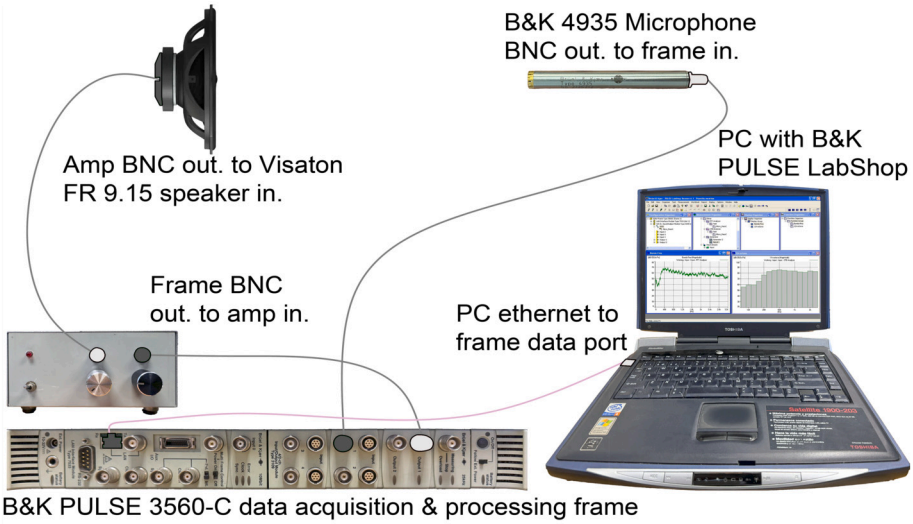

Fig. 6. Material and connection diagram of the equipment involved in the measurements of the experimental prototype.

2.4.1. Measurement set-up

The platform selected to perform the experimental measurement is a Brüel & Kjær PULSE Type 3560-C, with which both signal emission and reception are controlled.

Signal acquisition is carried out with a Brüel & Kjær type 4935 $^{1}/_{4}''$ microphone. To ensure steady-state measurement conditions, a continuous white noise signal is emitted from a Visaton FR 9.15 sound source during the measurements. Each measurement takes approximately one

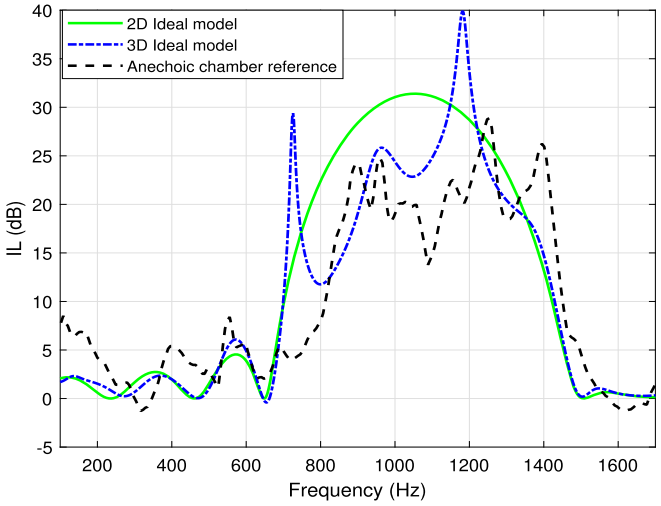

Fig. 7. IL spectra of the different numerical models in relation to the experimental measurement in anechoic chamber reference.

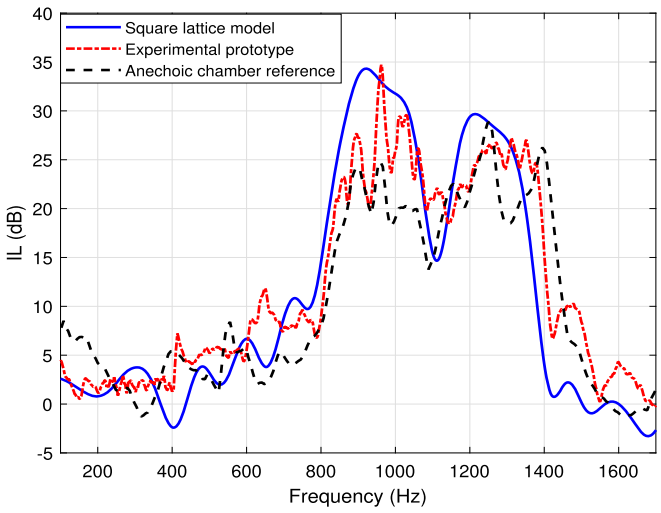

Fig. 8. IL spectra calculated with the proposed numerical model and experimentally measured on the prototype compared to the reference measurements made in the anechoic chamber.

minute with 1 000 FFT averages of the signal collected by the microphone (see Fig. 6).

3. Results and discussion

In this section we will first discuss the fitting capability of the different numerical models shown in the previous section 2.2 (the 2D and 3D ideal models) compared to the anechoic chamber measurement which is considered as a validation reference. For this purpose, a first simulation is made for a SC in a square lattice, with a lattice constant of 15 cm, trying to obtain a Bragg frequency in the traffic noise main frequency content.

As shown in Fig. 7, all models predict coincidentally the SCAS behaviour for the designed Bragg frequency. The 2D model gives a very clean view of the SCAS forbidden band and at the same time unrealistic, as it contemplates perfect theoretical assumptions of signal transmission. As an advantage, this model has a very low computational cost. On the other hand, the 3D model, with identical propagation and boundary conditions as the 2D model, incorporates effects derived from the height of the scatterers that bring us closer to the anechoic prediction while maintaining the correct location of the Bragg frequency.

In an attempt to bring some of the assumptions of the ideal model to a more realistic view, a new model is presented in which the emission is made by a point source closer to the emission characteristics of the loudspeaker used in the prototype. The lateral contours of periodic characteristics are replaced by a rigid boundary and the radiation conditions of the receiving chamber are replaced by PMLs.

The second result of interest is related to the agreement obtained between the proposed numerical model and the constructed experimental prototype with the anechoic measures.

As can be seen in Fig. 8, a significant agreement is achieved between the calculated numerical results and the measurements performed on the implemented prototype. The nature of the experimental results does not correspond as smoothly with the function obtained by the numerical method, obtaining a closer curve to the one measured in the anechoic chamber.

The experimental prototype IL results show a high degree of similarity in form and values with those measured in the anechoic chamber, improving in this aspect any of the numerical models analysed.

Finally, once both the new numerical prediction model and the experimental prototype have been validated, a study of a SCAS in triangular array with the same lattice constant is made.

In order to implement a triangular lattice on the prototype, the 20 cm tall circular scatterers have been precisely cut in half and glued by its edges to the side walls of the prototype using strong double-sided tape to seal them properly (see Fig. 9). The scatterers have been adjusted with precision in its position to match the numerical model.

The IL results of the experimental prototype show a high degree of similarity in shape and values between the prediction of the numerical model and the measurement performed on the experimental prototype in triangular lattice, as shown in Fig. 10. The perfect localization of the Bragg frequency is verified, although the width of the forbidden band decreases as expected. Lower IL values than those obtained in a square lattice are also observed, coinciding with what can be found in other works [23].

Although it is important to note that the prototype has limitations. The current design only allows measurement at one receiver point that can be moved closer to or further away from the last scattering surface, but does not support simultaneous measurement of a set of points. On the other hand, there are some discrepancies between the behaviour of the sample in the anechoic chamber and in the numerical models. These discrepancies can be due to several factors, such as (i) diffraction from the side or top and bottom edges of the sample or, (ii) to the difference in the consideration of the incident wave. We have tried to minimize this last case by placing the point source as far away from the sample as possible in the anechoic chamber, and assume that the incident wave on it is plane.

4. Conclusion

This paper presents a comprehensive model formed by a new numerical model and an experimental prototype for the analysis of the physics of SCs and for the design of acoustic barriers based on SCs in the low frequency regime. For the validation of the results, anechoic chamber measurements of the same modelled and tested SCs were performed, considering that the anechoic chamber reference result is more alike to the real behaviour of a barrier “in situ”.

The proposed numerical model is compared with the ideal models usually employed for prediction, working at a normal incidence and studying the attenuation properties of the SC in the low frequency regime. The proposed model breaks with the characteristics of the ideal models by trying to approximate to more realistic conditions that guide the construction of an experimental prototype. The outcomes obtained with the proposed model are more in line with the validation reference than those obtained with the ideal models. Based on the conditions established in this proposed prediction model, an equivalent SC to the one used in the reference measurements has been built and tested in

Fig. 9. Prototype with triangular lattice SC arrangement.

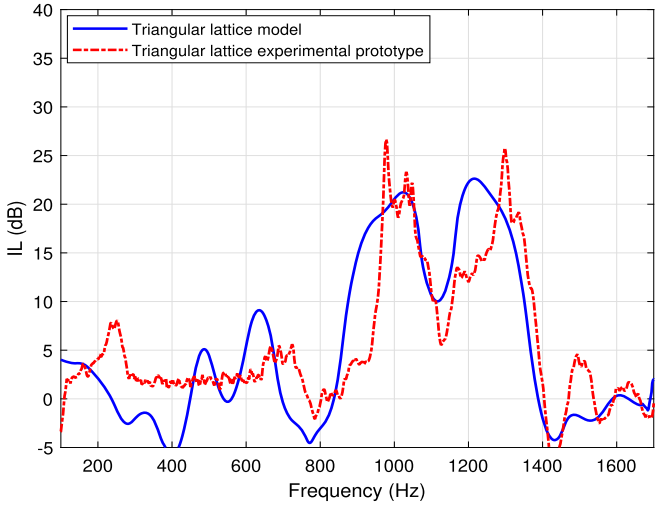

Fig. 10. IL spectra of the triangular lattice numerical model and the prototype.

an experimental prototype. The results achieve a more accurate fit than any of the numerical models. Its reliability is tested in both square and triangular lattice SCs.

In this work we have achieved good results in the IL prediction by replacing a set-up of 40 scatterers of 150 cm height, requiring exhaustive control of placement and parallelism, with a set-up of 4 scatterers of 20 cm in height. All of this leads to significant material savings, exceeding 98% in our experiment, thereby resulting in a significant reduction in costs and assembly complexity. The results obtained allow to work in a cheap and simple way, avoiding the need for large-scale tests in anechoic chambers. On the other hand, the use of our comprehensive model would allow other research groups that do not have access to an anechoic chamber to get a realistic view of the behaviour of their designs. The prototype is tested for actual scatterer diameters, rather than scaled ones, thus only limiting their height. This opens up the door to testing scatterers that can be 3D printed with designs that are more complex.

CRediT authorship contribution statement

L. Onrubia-Fontangordo: Writing – original draft, Validation, Software, Methodology, Investigation, Formal analysis. **J.M. Bravo Plana-Sala:** Writing – original draft, Supervision, Resources, Funding acquisition, Conceptualization. **S. Castiñeira-Ibáñez:** Writing – original draft, Validation, Methodology, Conceptualization. **J.V. Sánchez-Pérez:** Writing – original draft, Project administration, Methodology, Conceptualization.

Declaration of competing interest

The authors declare that they have no known competing financial interests or personal relationships that could have appeared to influence the work reported in this paper.

Data availability

Data will be made available on request.

References

[1] Thompson SD. Noise and vibration as elements of nuisance. Am Law Reg 1883;31(10):625. https://doi.org/10.2307/3304717.
[2] World Health Organization. Environmental noise guidelines for the European region. World Health Organization, Regional Office for Europe; 2018. https://www.who.int/europe/publications/i/item/9789289053563.
[3] European Environment Agency. Environmental noise in Europe – 2020. Publications Office; 2020.
[4] Houthuijs D, Swart W, van Kempen E. Implications of environmental noise on health and wellbeing in Europe. EIONET Report — ETC/ACM 2018/10, Tech. Rep., European Environment Information and Observation Network; 2018. https://eionet.europa.eu/etcs/etc-atni/products/etc-atni-reports/eionet_rep_etcacm_2018_10_healthimplicationsnoise.
[5] Blanes N, Fons-Esteve J, Hintzsche M, Ramos MJV, Röösli M, De La Maza MS, et al. Projected health impacts from transportation noise – exploring two scenarios for 2030. ETC HE Report 2022/5., Tech. Rep., 2022. https://doi.org/10.5281/zenodo.7361855.
[6] Praticò FG, Briante PG, Speranza G. Acoustic impact of electric vehicles. In: 2020 IEEE 20th Mediterranean electrotechnical conference (MELECON); 2020. p. 7–12.
[7] Ling S, Yu F, Sun D, Sun G, Xu L. A comprehensive review of tire-pavement noise: generation mechanism, measurement methods, and quiet asphalt pavement. J Clean Prod 2021;287:125056. https://doi.org/10.1016/j.jclepro.2020.125056.
[8] Ferrara A, Sicona S, Siri S. Freeway traffic modelling and control. https://doi.org/10.1007/978-3-319-75961-6, 2018.
[9] Van Renterghem T, Forssén J, Attenborough K, Jean P, Defrance J, Hornikx M, et al. Using natural means to reduce surface transport noise during propagation outdoors. Appl Acoust 2015;92:86–101. https://doi.org/10.1016/j.apacoust.2015.01.004.
[10] Laxmi V, Thakre C, Vijay R. Evaluation of noise barriers based on geometries and materials: a review. Environ Sci Pollut Res Int 2021;29(2):1729–45. https://doi.org/10.1007/s11356-021-16944-2.
[11] Maekawa Z. Noise reduction by screens. Appl Acoust 1968;1(3):157–73. https://doi.org/10.1016/0003-682x(68)90020-0.
[12] Martínez-Sala RM, Sancho J, Sánchez-Pérez JV, Gómez V, Llinares J, Meseguer F. Sound attenuation by sculpture. Nature 1995;378(6554):241. https://doi.org/10.1038/378241a0.
[13] Foldy LL. The multiple scattering of waves. I. General theory of isotropic scattering by randomly distributed scatterers. Phys Rev 1945;67:107–19. https://doi.org/10.1103/PhysRev.67.107.
[14] Gupta A. A review on sonic crystal, its applications and numerical analysis techniques. Acoust Phys 2014;60(2):223–34. https://doi.org/10.1134/s1063771014020080.
[15] Gieva E, Ruskova I, Nedelchev K, Kralov I. Comparative analysis of the acoustic efficiency of classical and sonic crystal noise barriers. IOP Conf Ser 2020;1002(1):012014. https://doi.org/10.1088/1757-899x/1002/1/012014.
[16] Qin X, Ni A, Chen Z, Fang M-J, Li Y. Numerical modeling and field test of sonic crystal acoustic barriers. Environ Sci Pollut Res Int 2022;30(6):16289–304. https://doi.org/10.1007/s11356-022-23109-2.
[17] Castiñeira-Ibáñez S, Rubio C, Romero-García V, Sánchez-Pérez JV, García-Raffi LM. Design, manufacture and characterization of an acoustic barrier made of multi-phenomena cylindrical scatterers arranged in a fractal-based geometry. Arch Acoust 2012;37(4):455–62. https://doi.org/10.2478/v10168-012-0057-9.
[18] Sánchez-Pérez JV, Rubio C, Martínez-Sala R, Sanchez-Grandia R, Gómez V. Acoustic barriers based on periodic arrays of scatterers. Appl Phys Lett 2002;81(27):5240–2. https://doi.org/10.1063/1.1533112.
[19] Morandi F, Miniaci M, Marzani A, Barbaresi L, Garai M. Standardised acoustic characterisation of sonic crystals noise barriers: sound insulation and reflection properties. Appl Acoust 2016;114:294–306. https://doi.org/10.1016/j.apacoust.2016.07.028.

[20] Romero-García V, Sánchez-Pérez JV, García-Raffi LM. Tunable wideband BandStop acoustic filter based on two-dimensional multiphysical phenomena periodic systems. J Appl Phys 2011;110(1). https://doi.org/10.1063/1.3599886.
[21] Romero-García V, Sánchez-Pérez JV, García-Raffi LM. Analysis of the wave propagation properties of a periodic array of rigid cylinders perpendicular to a finite impedance surface. Europhys Lett 2011;96(4):44003. https://doi.org/10.1209/0295-5075/96/44003.
[22] Castiñeira-Ibáñez S, Rubio C, Sánchez-Pérez JV. Environmental noise control during its transmission phase to protect buildings. Design model for acoustic barriers based on arrays of isolated scatterers. Build Environ 2015;93:179–85. https://doi.org/10.1016/j.buildenv.2015.07.002.
[23] D'Orazio T, Asdrubali F, Godinho L, Veloso M, Amado-Mendes P. Experimental and numerical analysis of wooden sonic crystals applied as noise barriers. Environments 2023;10(7):116. https://doi.org/10.3390/environments10070116.
[24] Berenger J-P. A perfectly matched layer for the absorption of electromagnetic waves. J Comput Phys 1994;114(2):185–200. https://doi.org/10.1006/jcph.1994.1159.